

Supplementary Information

Micro-engineered perfusable 3D vasculature for cardiovascular diseases

Nishanth Venugopal Menon,^a Hui Min Tay,^b Soon Nan Wee,^c King Ho Holden Li ^a and Han Wei Hou^{b*}

- ^a. School of Mechanical and Aerospace Engineering, Nanyang Technological University, 50 Nanyang Avenue, Block N3, Singapore 639798
- ^b. Lee Kong Chian School of Medicine, Nanyang Technological University, 11 Mandalay Road, Clinical Sciences Building Level 11, Singapore 308232.
Email: hwhou@ntu.edu.sg; Tel: +65 65923889
- ^c. School of Chemical and Biomedical Engineering, Nanyang Technological University, 62 Nanyang Drive, Singapore 637459.

Experimental section

Cell culture

Human Umbilical Vein Endothelial Cells (HUVECs, Lonza) and Aortic Smooth Muscle Cells (SMC, Lonza) were cultured using Endothelial Cell Growth Medium (EGM-2, Lonza) and Smooth Muscle Growth Medium (SmGM-2, Lonza) respectively, and passage numbers 4 to 8 were used for both cell lines. The cells were maintained at 37 °C in a humidified 5% CO₂ incubator and passaged every 4 days. Confluent layers were dissociated using 0.25% trypsin with 1 mM EDTA (Gibco). For on-chip culture, HUVECs were suspended to a concentration of 2×10^6 cells /mL and seeded into the top microchannel. The device was tilted from side to side and overturned, keeping it at each position for about 2 min, to facilitate cell distribution and cell attachment inside the channel. EGM-2 media was replenished every day.

Device characterization using capillary burst valve (CBV)

Channel width characterization was performed using straight channels with varying channel widths (100 μm, 200 μm, 500 μm and 1000 μm) and a fixed channel height (150 μm), while the channel height characterization was performed using straight channels with varying heights (25 μm, 100 μm, 150 μm) and a fixed channel width (500 μm). 100 nM of FITC was added to collagen gel and loaded into the device for visualization. The device was sliced along the width of the channel and the channel cross-section was sealed to a cover slip. Fluorescence images of the FITC-laden collagen were taken using an inverted fluorescence microscope (Nikon Eclipse Ti). The contact angle made by the advancing meniscus, with the channel surface and the bulging distances (along the center, D and along the bottom, d), were calculated from the fluorescence images using

ImageJ. The relationship between the bulging distances and the contact angle and force exerted ($P_s - P_o$) was calculated from the Young-Laplace equation (Equation S1).

$$P_s - P_o = -2\sigma \frac{\cos \theta_T}{h} \quad (S1)$$

Characterization of the chemoattractant concentration gradient

The characterization of the chemoattractant concentration gradient in the collagen gel was studied using 1 μ M FITC dye, which has a similar molecular weight to that of N-Formylmethionine-leucyl-phenylalanine (fMLP \sim 380 Da v.s. \sim 438 Da respectively). FITC dye was introduced into the gel ports of the ECM chamber and allowed to diffuse into the collagen towards the cell channel. Fluorescent images were taken at time 0 hr, 2 hr, 4 hr and 8 hr, and the corresponding fluorescent intensities were measured using linescan to determine the representative FITC concentration gradient.

Immunostaining and 3D cell imaging

For immunostaining, the cells (HUVECs and SMC) were fixed using 4% paraformaldehyde (Sigma Aldrich) for 15 min. The fixed samples were immunolabelled for VE-cadherin using rabbit anti-human CD144 primary antibody (10 μ g/mL, Enzo) and fluorescently labelled with AlexaFluor 488 goat anti-rabbit secondary antibody (20 μ g/mL, Santa Cruz Biotechnology). AlexaFluor 568 phalloidin (0.17 μ M, Life Technologies) and Hoescht 33342 (1 μ g/mL, Life Technologies) were used to stain for the cell cytoskeleton (F-actin) and nuclei respectively. The

3D organization of the cells inside the device was captured using a confocal microscope (Carl Zeiss LSM 800, Germany).

Author contributions

N.V.M, H.W.H and K.H.H.L designed research. N.V.M, H.M.T, S.N.W and H.W.H, performed experiments and analyzed the data. N.V.M, H.M.T and H.W.H wrote the manuscript. All authors reviewed the manuscript. The authors have declared that no conflict of interest exists.

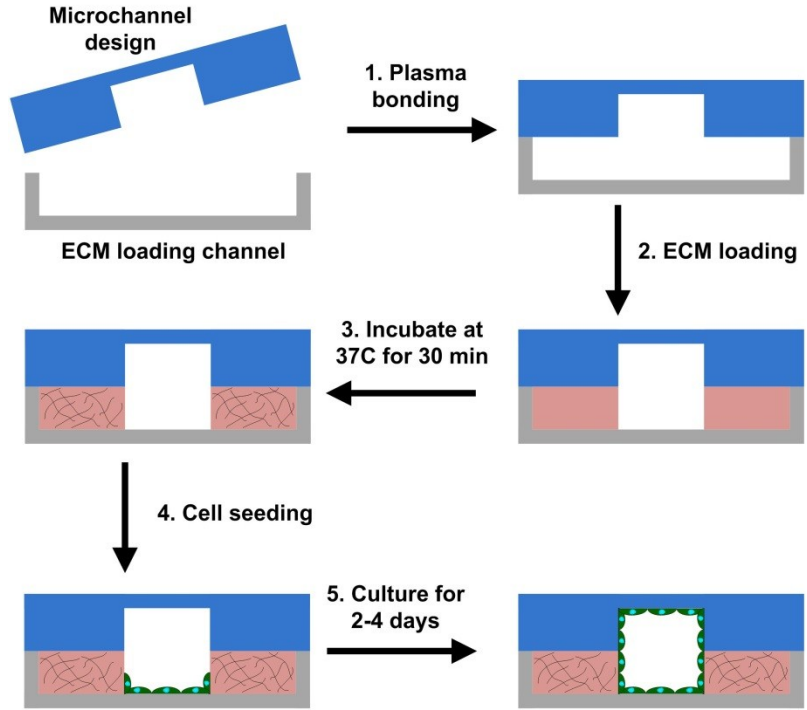


Figure S1: Device fabrication: Schematic illustration of the ECM loading procedure. ECM loading channel (bottom layer) and vascular microchannel design (top layer) are aligned and bonded together after plasma treatment. ECM is loaded through the bottom ports which would flow and stop at the boundaries defined by the microchannel top layer due to capillary burst valve (CBV). After incubation for 30 min at 37 °C, ECM is polymerized to form perfusable microchannels and vascular cells are seeded into the channels for cell culture.

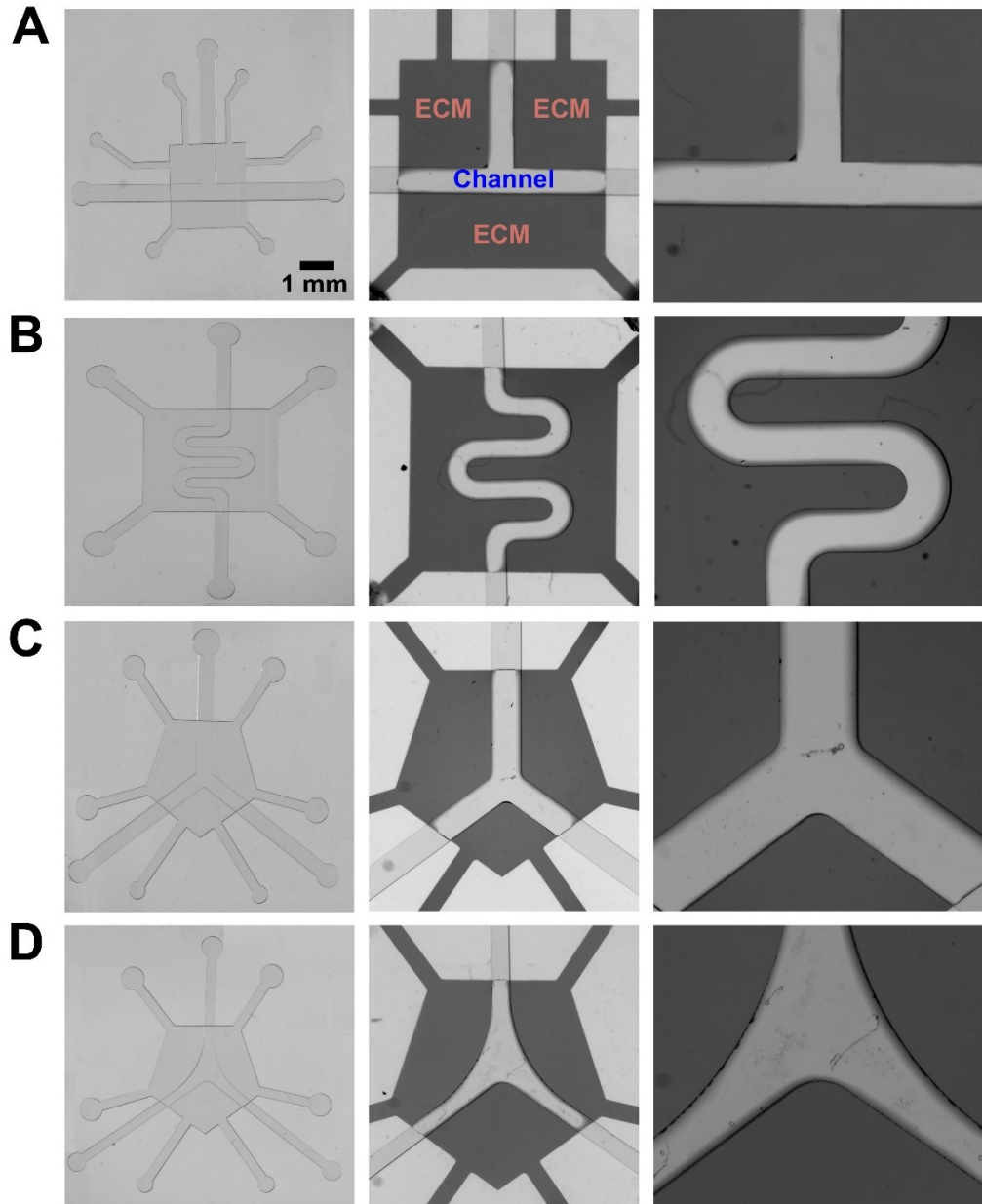


Figure S2: Geometric flexibility of the ECM patterning approach: Brightfield images showing ECM loading channels (bottom) aligned with different microchannel geometries for (A) T-junction, (B) serpentine, (C) Y-junction and (D) filleted Y-junction. Type I collagen (2.5 mg/mL) added with food dye was used to illustrate the hydrogel patterned microchannels. (Scale bar: 1 mm)

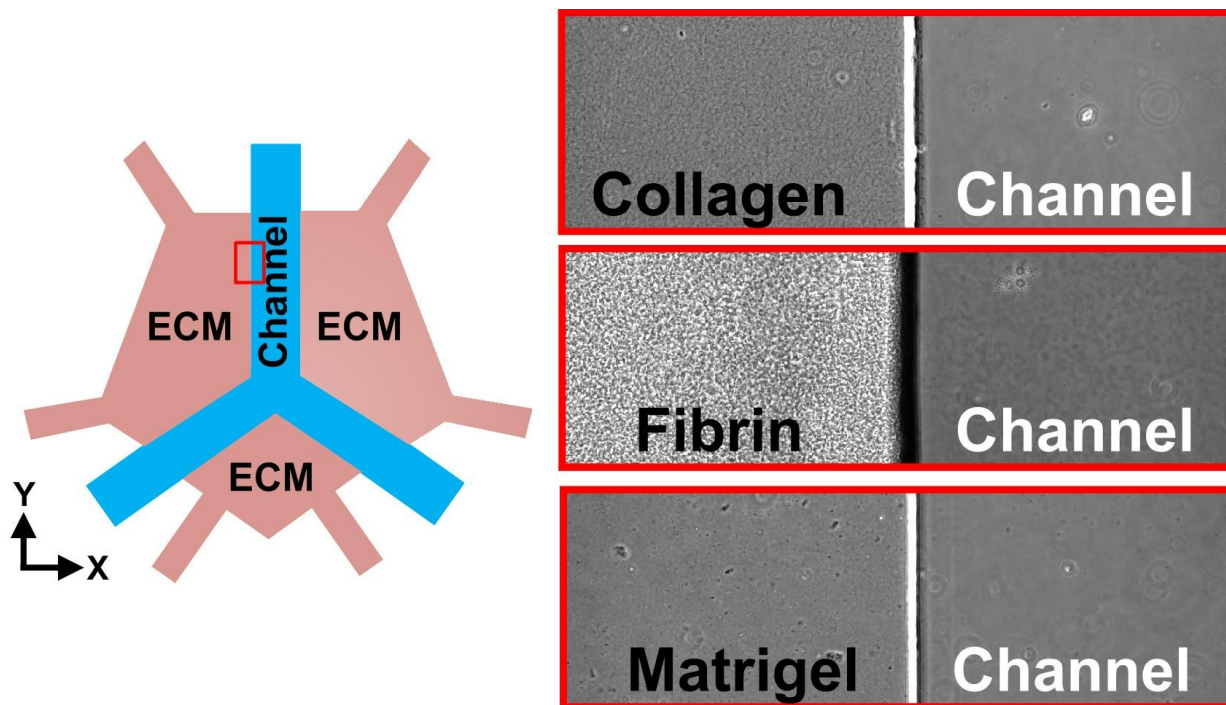


Figure S3: ECM patterning of different hydrogels: (Left) Schematic of a Y-channel microfluidic device. (Right) Magnified brightfield images of ECM patterns using collagen, fibrin and Matrigel.

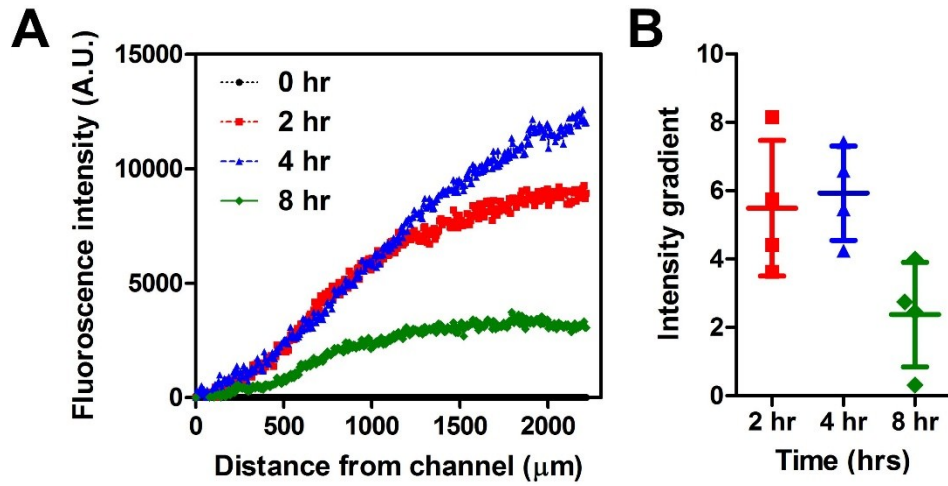


Figure S4: Characterization of chemoattractant-concentration gradient: (A) Plot illustrating the fluorescent linescan of 1 μM FITC dye in the collagen gel over different time points. All values are normalized to time T=0 hr. (B) Plot highlighting the slope of the gradient plot highlighting the creation of a stable gradient. n=4. Data are presented as mean \pm s.d.

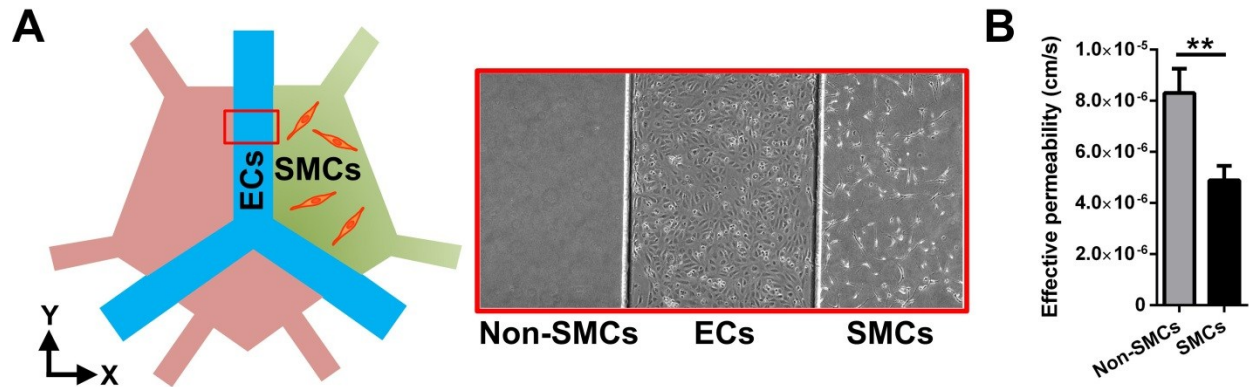


Figure S5: Effective barrier permeability of endothelial monolayer with and without aortic smooth muscle cells (SMC): (A) SMC are introduced into one side of the collagen gel, while the other side is kept without SMC. Inset shows the brightfield image of a section of the chip with SMC on one side of the HUVECs channel. (B) Barrier permeability of inflamed endothelium measured from either side of the HUVEC channel (n=4). SMC reduced the leakiness of the endothelial barrier. Data are presented as mean \pm s.d. (**p< 0.01).

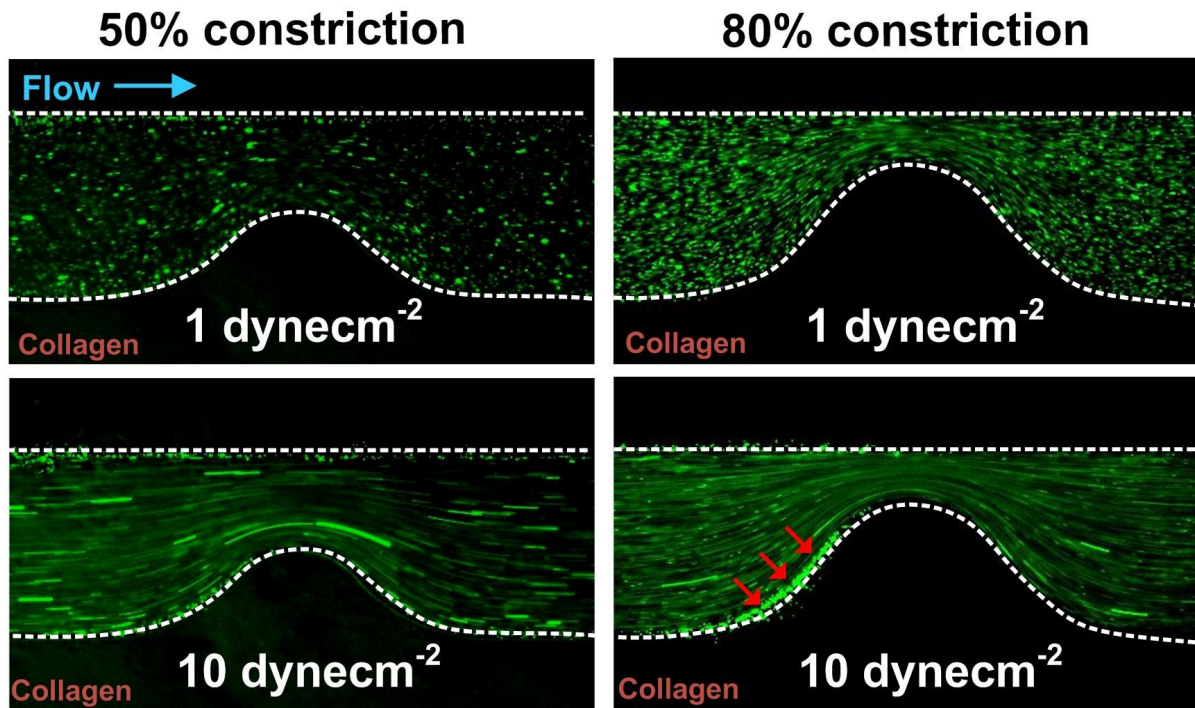


Figure S6: Flow profile at different ECM-patterned channel constrictions: Fluorescent images of FITC-conjugated 2 μ m beads at different flow rates in channels with different channel constrictions. No beads accumulation was observed for 50% constriction while at 10 dyne/cm^2 , beads accumulated (red arrows) for 80% constriction.

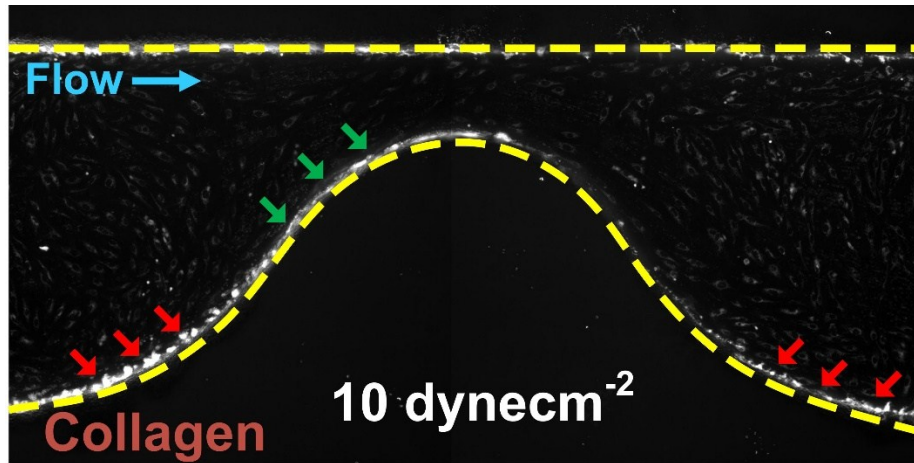


Figure S7: Differential platelets and leukocytes adhesion under whole blood perfusion (10 dyne/cm^2): In addition to platelets and leukocytes (R6G-stained) adherence at both proximal and distal regions (red arrows) of the collagen-patterned constriction (80%) due to low wall shear stresses, increased platelet binding (green arrows) was observed at the proximal region nearer the channel constriction with additional convective flow into the ECM (collagen).